Experimental comparison of canal models for control purposes using simulation and laboratory experiments

Klaudia Horváth, Eduard Galvis, José Rodellar and Manuel Gómez Valentín

ABSTRACT

Considerable amounts of water can be saved by automating irrigation canals. The design of most of the practical automatic controllers rely on a simplified model of the irrigation canal. This model can be obtained from measured data (identification) or can be formulated (white box models) assuming simplifications in the physical concepts and using the canal geometry. Several models of this kind are presently available. Moreover, short canals reveal a resonance problem, due to the back and forth of waves. This paper is focused on how to choose a suitable model for short canal pools with the purpose of control design. Four simple models are applied to two different types (resonant and non-resonant) of short canals: First order transfer function based on the Hayami model, Muskingum model, Integrator Delay (ID), and Integrator Delay plus Zero (IDZ). Model predictive controllers are developed based on these models and they are tested numerically and experimentally in order to evaluate their contribution to the control effectiveness. The controllers based on the ID and IDZ model showed the best performance.

Key words | automatic control, irrigation canals, laboratory flumes, models for control purposes, predictive control

Klaudia Horváth (corresponding author)
Manuel Gómez Valentín
Technical University of Catalonia,
Department of Environmental,
Hydraulic and Maritime Engineering,
C. Jordi Girona 1,
Barcelona 08034,
Spain
E-mail: *klaudia.horvath@upc.edu*

Eduard Galvis
José Rodellar
Technical University of Catalonia,
Department of Applied Mathematics III,
C. Jordi Girona 1,
Barcelona 08034,
Spain

NOMENCLATURE

Latin letters

A (m^2)	cross-sectional area
A_e (m^2)	storage surface
$A_{e\mathrm{ID}}$ (m^2)	the backwater area for the ID model
$A_{e\mathrm{IDZ}}$ (m^2)	backwater area for the IDZ model
B_g (m)	width of the gate
B (m)	bottom width
C_0 (m/s)	celerity coefficient
C_dg ($-$)	gate discharge coefficient
C_dw ($-$)	weir discharge coefficient
$\mathrm{C_L}$ ($-$)	constant in the Hayami model moment matching
D_0 (m^2/s)	diffusivity coefficient
e (m)	water level error
G_FO	transfer function of the first order model between water levels
$G_{\mathrm{FO}q}$	transfer function of the first order model between discharges
G_M	transfer function of the Muskingum model between water levels
$G_{\mathrm{M}q}$	transfer function of the Muskingum model between discharges
H (m)	downstream water level
H_2 (m)	water level downstream the gate
h_sp (m)	water level setpoint
K (s)	storage time constant
K_1 (s)	time constant of the first order model
k_hg	gain of the gate discharge
k_hw	gain of the weir discharge
K_IDZ1	a parameter of the IDZ model

doi: 10.2166/hydro.2014.110

K_{IDZ2}	a parameter related to the IDZ model
L (m)	length of the canal pool
L_g (m)	gate opening
L_w (m)	width of the weir
m (-)	side slope of a channel
n ($m^{-1/3}$/s)	Manning's coefficient
O (m)	the height of the weir
P	weighting matrix for the water level error
q_{in} (m^3/s)	relative input discharge
Q_{in} (m^3/s)	input discharge
Q_{in0}	steady state input discharge
Q_{off} (m^3/s)	offtake discharge
Q_{out} (m^3/s)	output discharge
Q_t (m^3/s)	transport discharge
R	weighting matrix for the change in input discharge
R_h (m)	hydraulic radius
S_b (m/m)	bottom slope
S_f (-)	friction slope
T_w (m)	width of the free surface
u	input control vector
V (m^3)	storage volume
v_{sto}	relative storage volume
W	disturbance vector
x	the state vector

Greek letters

η (−)	dimensionless characteristic of the length of the canal pool
λ (−)	prediction horizon
σ (−)	dimensionless characteristic of the wave propagation in a canal pool
τ_{ID} (s)	the time delay for the ID model
τ_{IDZ} (s)	the time delay for the IDZ model
χ (−)	Muskingum model coefficient

Acronyms

ID	Integrator Delay
IAE	Integral of absolute magnitude of error
IDZ	Integrator Delay Zero
MAE	Maximum absolute error
MUS	Muskingum
FO	first order
ASCE	American Society of Civil Engineers
SCADA	Supervisory Control and Data Acquisition System
SIC	simulation of irrigation canals
StE	steady state error
TSS	time to reach steady state indicator
UPC-PAC	(Canal de Prueba de Algoritmos de Control – Universitat Politècnica de Catalunya) Technical University of Catalonia – Control Algorithms Test Canal

INTRODUCTION

Irrigation is one of the largest water users, and given the increasing water stress, there is demand for more efficient management. Automatic control of irrigation canals is one of the ways to achieve this efficiency, aiming to reduce water losses while increasing economical and ecological benefits. The goal of automatic canal operation is to deliver the right amount of irrigation water in the right time, allowing on-demand operation of irrigation canals. The control of the canals is implemented by means of programmable automatic controllers that are able to control from a single canal pool to a whole network of irrigation canals.

One of the control techniques applied for irrigation canals (Rodellar *et al.* 1989; van Overloop 2006; van Overloop *et al.* 2010a) is model predictive control (MPC). This control technique is based on a suitable system model that must be accurate enough to capture significant dynamic behavior and simple enough for allowing online optimization. In the case of MPC, optimization is carried out online at every time step. By using linear models, this means solving a quadratic programming problem. However, in the case of nonlinear model predictive control (NMPC) a nonlinear problem has to be solved, which is computationally expensive (Schwanenberg *et al.* 2010a). There are existing studies about NMPC of water systems (Igreja & Lemos 2009; Schwanenberg *et al.* 2010b), but the majority

of MPC for water systems are still using linearized models or multiple model approaches (van Overloop *et al*. 2008). Since this work focuses on the use of linear MPC, only linear models are considered in the following.

Several surveys are available about irrigation canal models for control purposes. Malaterre & Baume (1998) categorized canal models of finite and infinite order, linear and nonlinear models. Zhuan & Xia (2007) categorized the models based on the way they are obtained: black and white box models. Malaterre (2008) summarized the existing models including both categories, presenting also a discussion about them. Mareels *et al*. (2005) raised the question of the possible level of discretization and simplification that can be used for models for controller design. However, comparative evaluations between these models are missing. In the following, some existing hydraulic models are briefly introduced.

These simple models can be categorized into three different groups based on the way they are obtained. Black box refers to models obtained by using system identification without using physical knowledge of the system. Gray box models (Refsgaard 1996) have a structure based on physical knowledge and their parameters are identified from measured data. In a third group, white box models do not need any measured data, and they are proposed from the canal geometry using conservation laws (storage equations, for instance). The advantage of black box models is their simplicity: only experimental data are taken and a model can be fitted without assuming knowledge of the system dynamics. The disadvantage of this method is that the model structure might not take into account the real dynamics. It might be different from the real process, especially in operation points further from the point where the data set for the identification was collected. Moreover, in some cases it may not be possible to collect data or the collection of the data may be very expensive. This methodology is often used in control problems. It has been applied to laboratory canals: for instance, in Sepúlveda (2008), ARX (AutoRegresive with eXternal input) models were identified with orders between 5 and 10; and second and third order models were identified in Begovich *et al*. (2007). Linear first order (FO) models with varying parameters were applied for the Lunax dam-gallery at Gascogne by Puig *et al*. (2005). In van Overloop & Bombois (2012), the authors identified a ninth order model from experimental data using an existing canal at the Central Arizona Irrigation and Drainage District.

In the case of gray box models, the model dynamics is a priori given, but the parameters are identified using experiments and operational data. The following are examples of models of different structures: third order in Weyer (2001); FO with delay in Aguilar *et al*. (2009, 2011); and Integrator Delay plus Zero (IDZ) model in Aguilar *et al*. (2012). In Duviella *et al*. (2013), a multivariable state space model containing delays is identified. It is possible to obtain the parameters by open (Eurén & Weyer 2007) or closed loop identification (Ooi & Weyer 2001).

The white box models are based on the mathematical description (conservation laws) of the system. There are models with different complexities, but all of them can be derived from the Saint–Venant (SV) equations. The advantages of this approach are that the model contains the real dynamics of the system, it might have a wider range of validity, and it does not require measurements. However, these models may not be simple to establish, and the dynamics of the complete system may not be known in all the cases. Or, even sometimes, the whole system is so complicated that there is a need for simplification of the original model.

One possible way to obtain linear models for control purposes is to linearize the SV equations. However, the linearized SV equations are still partial derivative equations, which need special treatment for controller design (Malaterre & Rodellar 1996). When the SV equations are discretized, e.g., with the Preismann scheme, a spatial discretization is needed. This, depending on the scale of the space discretization, can increase considerably the size of the system. There are some models obtained from the linearization of the SV equations in the uniform regime. However, in the case of irrigation canals the flow is often affected by backwater due to the presence of hydraulic structures, therefore the use of simple models that are able to represent this condition is beneficial (Litrico & Fromion 2004c).

A simplified SV model is presented by Xu *et al*. (2011), comparing it to the whole SV model and analyzing the differences and computation times. Simplified versions of these equations have been proposed, for example the diffusive wave equations, which with the help of the moment

matching method can be approximated as second order model with delay (Malaterre 1994; Litrico & Georges 1999). Simplified hydraulic models like the Muskingum model have been used by some authors (Rodellar *et al.* 1989; Gómez *et al.* 1998; Alvarez Brotons 2004). Another simplified hydraulic model, the Hayami model, is also used for control purposes by Chentouf (2001) and Charbonnaud *et al.* (2011).

The most common simplified model used in practice is the Integrator Delay (ID) model: (van Overloop *et al.* 2005, 2010a; Wahlin & Clemmens 2006; Zafra-Cabeza *et al.* 2011). The IDZ model is the extension of the ID model. Another model in the literature developed for control purposes, but not used at the time this work was carried out, is the Integrator Resonance model (van Overloop *et al.* 2014).

The choice between black or white box models often depends on the available data and knowledge about the canal. However, once white box models have been decided upon, there is no study about how to choose a particular model within this group. The initial choice might depend on the type of control one would like to apply and also the canal type. In this study, we search for the answer to this question for a specific canal type: short canals. The aim of this work is to find out which white box model would be the best choice as internal model for MPC for short canals.

The working methodology is as follows: some simple models from the literature are reviewed and implemented for two different canals. They are compared in both time and frequency domain as a preliminary test. Predictive controllers are developed based on them and tested numerically. The best performing controllers are implemented experimentally in the laboratory canal of the Technical University of Catalonia. The influence of the model choice on the controller performance is assessed. The two cases studied in this paper are representative of two classes of typical canals characterized in the irrigation canal control area.

The paper is organized as follows. First, the examples for the two canal types are described: the laboratory canal of the UPC, which is as an experimental facility, and the Corning canal, which is used in numerical simulations. Second, the different canal models are described and analyzed in the time and frequency domain. Third, the MPC development is described. Fourth, the numerical and experimental results of the controllers are analyzed and, finally, conclusions are drawn.

THE LABORATORY CANAL OF THE TECHNICAL UNIVERSITY OF CATALONIA

The UPC-PAC canal (Canal de Prueba de Algoritmos de Control – Universitat Politécnica de Catalunya) is specially designed to develop basic and applied research in the field of control of irrigation canals. The canal is designed with a serpentine shape in order to achieve the greatest length using a small surface area. The shape might have some effects on the flow characteristics, but these are especially local effects, like the turbulences occurring at the curves that might increase the energy losses. The laboratory canal with its time delay can be used to test canal control algorithms (Sepúlveda 2008). It has zero bottom slope in order to achieve the largest possible time delay. The geometrical data are summarized in Table 1. At the upstream end, there is a constant depth reservoir that is connected with a sluice gate to the canal.

The canal contains four operative motorized sluice gates, therefore it is possible to divide it into four pools. At the downstream end, there is a sharp crested weir with variable height. Gravity offtakes (lateral weirs with minimum height of 34.3 cm) are found at the downstream end of every pool. The maximum discharge that can circulate is 150 L/s. The UPC-PAC is short, completely affected by backwater. Due to the low friction and the zero slope, one wave can travel back and forth several times before it finally dampens. This phenomenon is known as

Table 1 | Geometrical data of the Corning and the laboratory canal where n is Manning's roughness coefficient, B is the bottom width of the canal, S_b is the bottom slope, L is the length, m is the side slope, Q_0 is the reference discharge and H_0 is the reference (downstream) water depth

	n ($m^{-1/3}/s$)	B (m)	S_b (-)	L (m)	m (-)	Q_0 (m^3/s)	H_0 (m)
UPC-PAC	0.016	0.44	0	220	0	0.07	0.65
Corning	0.02	7	0.0001	7000	1.5	11	2.1

resonance. A detailed description of its main features can be found in van Overloop *et al.* (2010b).

According to the Cemagref benchmark characterization (Baume *et al.* 1998), the UPC-PAC lies within the so-called Type 1: short canals having FO response with resonance. The Cemagref benchmark characterization is based on the use of two dimensionless variables, σ and η. Variable σ is a dimensionless length characteristic of the pool, which is also influenced by the normal depth, hence the normal flow. Variable η depends on σ and the Froude number. It is shown (Baume & Sau 1997) that σ characterizes the wave propagation and η characterizes the downstream level perturbations. The value of η shows if a wave is damped or not, and the value of σ shows the order of the wave model. These parameters are associated with the flow regime, and with a very different operational discharge the canal might fall into another category.

THE CORNING CANAL

The Corning canal is one of the test canals proposed by the American Society of Civil Engineers (ASCE) to test control algorithms (Clemmens *et al.* 1998). In this work, the first pool of this canal is used, which is bounded by a constant depth reservoir upstream and by a sluice gate downstream. This canal pool is relatively short, belonging to Type 3 in the Cemagref benchmarks. It is a short canal with FO behavior, that is a FO transfer function is used to relate the upstream and the downstream discharges. It shows no resonance phenomena. The geometrical data of this canal are shown in Table 1.

THE CANAL MODELS

In this section, first we give a general introduction to an example canal pool, then each model is described, finally the calculated parameters for each model for both canals are given.

In this work, a single canal pool is considered as case study, as illustrated in Figure 1. The canal is represented with two zones: transport and storage. The dynamics of the two parts are considerably different, and this distinction was first proposed by Schuurmans (1997). The main variables are Q_{in} (m^3/s) input discharge, Q_t (m^3/s) transport discharge (the discharge at the end of the transport zone), Q_{out} (m^3/s) output discharge, H (m) downstream water depth, Q_{off} (m^3/s) offtake discharge. The models are linearized around a steady state. In all cases, the absolute quantities are noted with capital letters, the steady state values have a zero index, and the values relative to the steady state are noted with small letters. For example, the relative input discharge is

$$q_{in}(t) = Q_{in}(t) - Q_{in0}. \quad (1)$$

The control objective is to keep the downstream water depth as close as possible to its prescribed setpoint by manipulating the input discharge through the upstream gate.

Muskingum model

The Muskingum model (abbreviated MUS in the following) is a frequently used linear model for flood routing (Cunge 1969). It has been also used for control purposes (Rodellar

THE CANAL MODELS

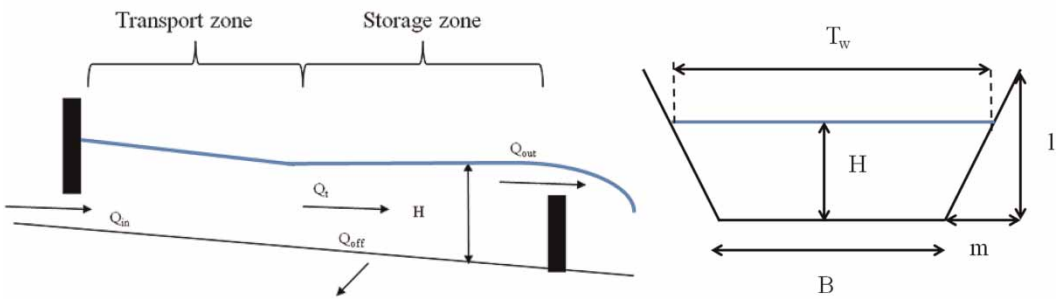

Figure 1 | Distribution of a canal pool into two zones and the trapezoidal cross section.

et al. 1993; Gómez et al. 1998; Mantecón et al. 2002). Simplicity and linearity are its main advantages.

The model consists of two equations, describing water storage and continuity, respectively

$$v_{\text{sto}}(t) = K[\chi q_{\text{in}}(t) + (1-\chi)q_{\text{t}}(t)] \tag{2}$$

$$\frac{\mathrm{d}v_{\text{sto}}}{\mathrm{d}t} = q_{\text{in}}(t) - q_{\text{t}}(t) \tag{3}$$

where v_{sto} is the relative storage volume, K is the storage time constant, and χ is a dimensionless coefficient. The storage time constant (with the dimension of time) can be well approximated by the time it takes for one wave to travel through the pool. Parameter χ is dimensionless and weighs the relative effects of inflow and outflow on the pool storage (boundary conditions), which varies in the range [0, 0.5]. It can be approximated from the flow and geometrical properties of the canal (Cunge 1969). Applying the Laplace transform to the model above, the following transfer function can be derived:

$$G_{\text{M}q}(s) = \frac{q_{\text{t}}(s)}{q_{\text{in}}(s)} = \frac{1 - K\chi s}{1 + K(1-\chi)s}. \tag{4}$$

In this paper, for simplicity reasons, the same notation is used to express a time function or its corresponding Laplace transform, for example $q_{\text{t}}(t)$ or $q_{\text{t}}(s)$. Details about the derivation of this transfer function can be found in Rodellar et al. (1989). This transfer function shows the relationship between the upstream discharge and the discharge at the end of the transport zone. In this work, the objective is to control the downstream water depth, hence there is a need for a transfer function between the upstream discharge and the downstream water depth. The storage zone can be modeled, if no offtake is present, as a tank in the form

$$A_e \frac{\mathrm{d}h}{\mathrm{d}t} = q_{\text{t}}(t) - q_{\text{out}}(t) \tag{5}$$

where A_e is the storage surface. It can be approximated as

$$A_e = T_{\text{w}} L, \tag{6}$$

where L is the length of the canal pool. Applying the Laplace transform, the following expression is obtained:

$$q_{\text{t}}(s) = sA_e h(s) + q_{\text{out}}(s). \tag{7}$$

By combining Equations (4) and (7), the transfer function between the upstream discharge and downstream water depth is the following:

$$G_{\text{M}}(s) = \frac{h(s)}{q_{\text{in}}(s)} = \frac{1 - K\chi s}{A_e s + K(1-\chi)A_e s^2}. \tag{8}$$

Hence, the downstream water depth can be expressed as

$$h(s) = G_{\text{M}}(s) q_{\text{in}}(s) - \frac{1}{A_e s} q_{\text{out}}(s). \tag{9}$$

FO model based on the Hayami equation

The Hayami model (Hayami 1951) is the linearization of the diffusive wave equation with the hypothesis that the celerity and diffusivity are constant

$$\frac{\partial q}{\partial t} + C_0 \frac{\partial q}{\partial x} - D_0 \frac{\partial^2 q}{\partial x^2} = 0 \tag{10}$$

where q is the relative discharge (deviation from the steady state discharge Q_0), C_0 is the celerity coefficient, and D_0 is the diffusivity coefficient. For trapezoidal channels (see Figure 1) these coefficients are:

$$C_0 = \frac{5Q_0}{3A_0} - \frac{2Q_0 m}{T_{\text{w}0}^2} \tag{11}$$

$$D_0 = \frac{Q_0}{2T_{\text{w}0}S_{\text{f}0}} \tag{12}$$

where $S_{\text{f}0}$ is the friction slope which can be calculated from Manning's equation

$$S_{\text{f}0} = \frac{Q_0^2 n^2}{A_0^2 R_{\text{h}0}^{4/3}} \tag{13}$$

where R_{h0} is the hydraulic radius. Manning's coefficient is obtained from the literature (Chow 1959). The use of the Hayami model has been studied for different control methods, such as feedforward control (Sawadogo 1992) and predictive control (Charbonnaud *et al*. 2011).

One of the ways to obtain a simple linear model from the Hayami equation is the momentum matching method (Malaterre 1994; Litrico & Georges 1999). (Detailed description of the method to obtain the transfer function can be found in these references, but here just a brief summary is given.) The concept is to make equal the low order moments of the Taylor expansion of the Laplace transforms of the calculated transfer function of the Hayami model and the first or second order function with delay. The low order moments correspond to low frequencies (s close to 0), which is the most common in natural systems. Depending on the canal properties, three different categories can be established. The following dimensionless coefficient is derived to characterize the canal pool:

$$C_L = \frac{C_0 L}{2D_0}. \tag{14}$$

Category 1: If $C_L > 9/4$, the pool is relatively long, a second order function with delay can be defined.

Category 2: If $1 < C_L \leq 9/4$ the pool is relatively small. The second order transfer function with delay is unstable, therefore it is possible to define a FO or a second order transfer function. In this case it is possible to equate the first three moments.

Category 3: When $C_L \leq 1$ the pool is very short. FO transfer function can be defined by equating the first two moments.

An analysis about canals falling into each category with different length and discharge can be found in Alvarez Brotons (2004). Both canals studied in this paper fall into Category 3, therefore a FO transfer function without delay can be defined:

$$G_{FOq}(s) = \frac{q_t(s)}{q_{in}(s)} = \frac{1}{1 + K_1 s} \tag{15}$$

where

$$K_1 = \frac{L}{C_0}. \tag{16}$$

In the remainder of this paper, this model will be referred to as FO model.

Just as in the case of the Muskingum model, by combining Equations (7) and (15) the relationship between upstream discharge and downstream water depth can be given in the form

$$G_{FO}(s) = \frac{h(s)}{q_{in}(s)} = \frac{1}{A_e s + A_e K_1 s^2} \tag{17}$$

and the downstream water depth can be expressed as

$$h(s) = G_{FO}(s) q_{in}(s) - \frac{1}{A_e s} q_{out}(s). \tag{18}$$

The Integrator Delay model

The ID model was developed by Schuurmans (1997) and it is widely used for water systems (Wahlin & Clemmens 2006; van Overloop *et al*. 2010a). The model is also based on the division of the canal pool into an upstream and a downstream part. The upstream part is characterized by uniform flow, while the downstream part is characterized by backwater. Some canals are completely affected by backwater, like the laboratory canal used in this study. In the backwater part, the dynamics is complicated: waves are travelling up and down and being reflected. However, in low frequencies the water depth behaves as an integrator of the discharge. Therefore the water depth can be approximated as the integral of the flow. The model is then defined in the form (Schuurmans 1995)

$$h(s) = \frac{1}{A_{eID} s} e^{-\tau_{id} s} q_{in}(s) - \frac{1}{A_{eID} s} q_{out}(s) \tag{19}$$

where τ_{id} is the time delay, q_{in} is the upstream discharge, q_{out} is the downstream discharge, and $1/A_{eID}$ is the gain of the integrator (backwater area). The first term of Equation (19) accounts for the effect of the upstream discharge to the downstream water level, the second term accounts for the effect of the downstream discharge (with negative sign because this is the discharge leaving the canal). The backwater area can be approximated using the surface of the

canal pool

$$A_{e\mathrm{ID}} = T_{\mathrm{w}} L. \tag{20}$$

If the water surface is close to horizontal this approximation is close to the real backwater surface.

Integrator Delay Zero model

Similar to the ID model, the IDZ model (Litrico & Fromion 2004a) is an extension of the ID model that includes a zero in the transfer function. It is able to represent the canal behavior in low and high frequencies; the integrator delay accounts for low frequencies, whereas the zero represents the direct influence of the discharge on the water depth in high frequencies. The IDZ model was derived from the linearization of the SV equations. The upstream (uniform) part and the downstream (backwater) part are modeled separately, then the two models are interconnected. The final form of the model is the result of the connections of these two models. The downstream water depth can be expressed in the form (Litrico & Fromion 2004a):

$$h(s) = \frac{K_{\mathrm{IDZ1}} s + 1}{A_{e\mathrm{IDZ}} s} e^{-\tau_{\mathrm{IDZ}} s} q_{\mathrm{in}}(s) - \frac{K_{\mathrm{IDZ2}} s + 1}{A_{e\mathrm{IDZ}} s} q_{\mathrm{out}}(s) \tag{21}$$

where K_{IDZ1} and K_{IDZ2} are parameters related to the zero calculated from the canal properties, τ_{IDZ} is the time delay, and $A_{e\mathrm{IDZ}}$ is the integrator/backwater area approximation. The structure of this model is similar to Equation (19) but extended with a zero. More details are given about the IDZ model in Appendix A (available online at http://www.iwaponline.com/jh/016/110.pdf). The detailed derivation of these transfer functions can be found in Litrico & Fromion (2004a, 2004c).

The parameters of the four models for both canals are given in Table 2.

COMPARISON OF THE MODELS IN THE TIME AND FREQUENCY DOMAINS

In order to understand the behavior of different models they are compared in time and frequency domains. The time domain analysis is often used for models developed for simulation purposes. The step response of these models is compared to real data or response of already existing models (Litrico & Fromion 2004c). The frequency domain analysis is used in the control field (Ogata 2010). By studying the bode diagram, the response of the model for different frequency excitations can be read, in other words, the response for different frequencies of the wave movement in the case of open channels. The knowledge of the frequency behavior is crucial when controllers are designed (Schuurmans 1997; van Overloop 2006).

In the time domain, the response of the downstream discharge to a step input in the upstream discharge is analyzed. In the frequency domain, the relation between the downstream depth and the upstream discharge is studied. The use of the downstream depth in modeling is particularly relevant for the automatic control problem.

Comparison of the transport part

The step response is calculated for the four models and compared to the numerical solution of the SV equations. The downstream boundary condition was the hydraulic structure: a weir for the UPC-PAC and gate for the Corning canal.

Figures 2 and 3 show the response for the Corning canal and the laboratory canal, respectively. The difference between the two canals can be seen in the step response of the SV equations: while the response of the Corning canal (Figure 2) looks like a FO, the response of the laboratory canal (Figure 3) looks like a FO response with a zero (the fast increase in the beginning of the response).

Table 2 | The parameters of the four different models for the Corning and the laboratory canal (UPC-PAC)

	Muskingum		Hayami				ID		IDZ			
	K (s)	X (-)	K_1 (-)	D_0 (m²/s)	C_0 (m/s)	C_L (-)	$A_{e\mathrm{ID}}$ (m2)	τ_{ID} (s)	τ_{IDZ} (s)	$A_{e\mathrm{IDZ}}$ (m²)	K_{IDZ1} (–)	K_{IDZ2} (–)
UPC-PAC	79.4	0.01	539	–	0.41	0.00	96.8	79.4	78.6	90.6	82.4	85.5
Corning	1385	0.10	10,393	4135	0.67	0.57	93,100	1385	1489	61,212	371	1472

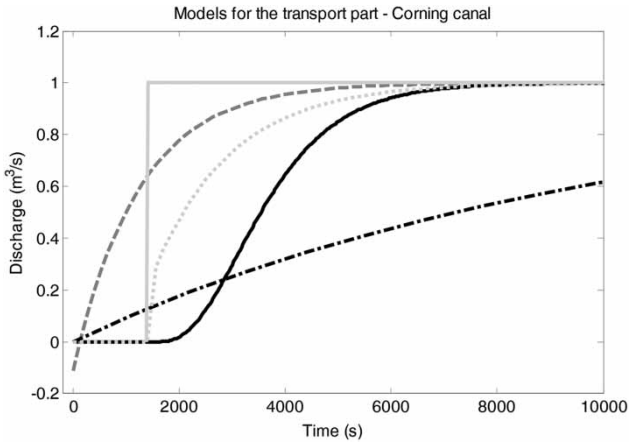

Figure 2 | Step response of the simple models of the Corning canal compared to the numerical solution of the SV equations: SV model (solid black line), ID model (solid gray line), IDZ model (dotted gray line), Muskingum model (dashed gray line), and the FO model (dash-dot line).

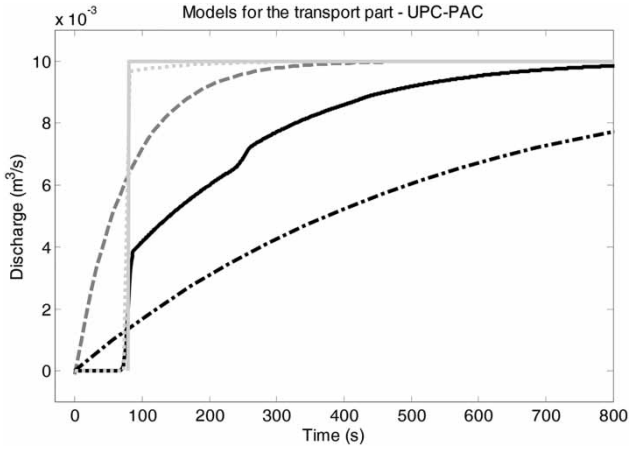

Figure 3 | Step response of the simple models of the UPC-PAC compared to the numerical solution of the SV equations: SV model (solid black line), ID model (solid gray line), IDZ model (dotted gray line), Muskingum model (dashed gray line), and the FO model (dash-dot line).

The ID model is a simple step with a time delay. Therefore its response is a pure step that starts at a time instant equal to the time delay of the SV model and the step size is equal to the peak response of the SV model. The ID and the IDZ models capture the time delay, which is correctly approximated as compared to the SV model. The difference between ID and IDZ is that IDZ has a shape more similar to the SV response: it captures this fast increase but deviates from SV in the whole transient period. This suggests the idea that IDZ should perform better than ID.

The response of the Muskingum and FO models contain no time delay. These models might compensate the delay with their slower behavior, but this might cause problems when controllers are developed. The response of the FO model is far from the response of the SV equations. The response of the Muskingum model is somewhat better. It is important to note that this model starts in the negative direction before increasing (Figure 2). This is due to the unstable zero in the transfer function in Equation (4). However, for controller design, it is better to approximate the frequency response of the system than its time response (Zhou & Doyle 1998).

Comparison in the frequency domain

The frequency response shows the response of the system when the input is a sinusoidal wave. The phase plot shows the change in the phase of the input wave, while the gain plot shows the change in the amplitude of the wave. The frequency responses of the Corning (Figure 4) and the laboratory canal (Figure 5) were obtained using the approximation method of Litrico & Fromion (2004b) to solve numerically the linearized SV equations. In this case, constant discharge as a downstream boundary condition was assumed.

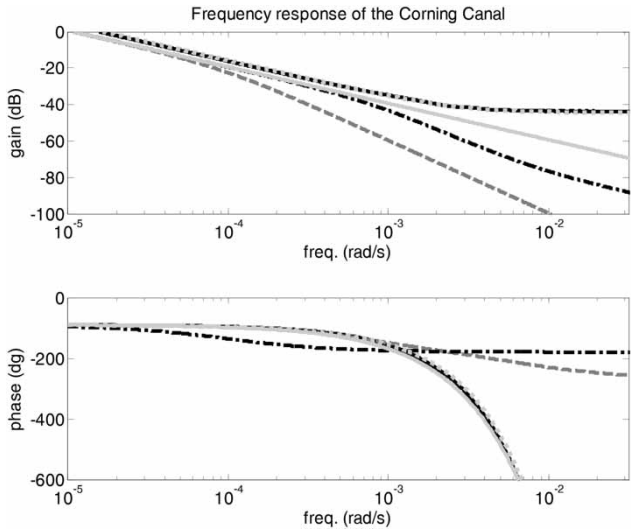

Figure 4 | Bode plot of the simple models of the Corning canal compared to the numerical solution of the SV equations: SV model (solid black line), ID model (solid gray line), IDZ model (dotted gray line), Muskingum model (dashed gray line), and the FO model (dash-dot line).

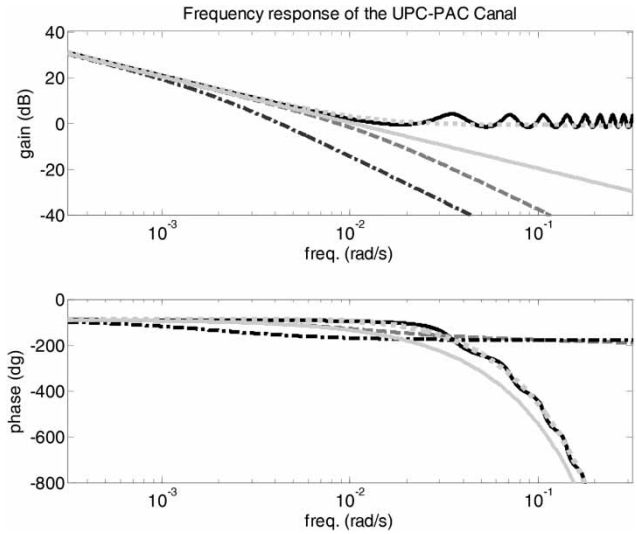

Figure 5 | Bode plot of the simple models of the UPC-PAC compared to the numerical solution of the SV equations: SV model (solid black line), ID model (solid gray line), IDZ model (dotted gray line), Muskingum model (dashed gray line), and the FO model (dash-dot line).

All the models in this comparison have two parts: transport and integrator. The FO and the Muskingum model only describe the transport part; they give a formula for the relationship between the upstream and the downstream discharges. In the case of the ID model, it can be assumed that a canal pool is divided into two sections: a transport zone and a backwater zone. The transport zone can be modeled using FO or Muskingum model and the backwater zone can be modeled as an integrator.

The gain response for the SV model shows a straight line in the low frequencies, when the system acts as an integrator: the water depth is the integral of the discharge. The line becomes horizontal at higher frequencies, which shows the presence of a zero in the transfer function. In the case of the laboratory canal, some peaks can be seen for high frequencies. These are resonance peaks: the water depth is changing as a wave is travelling back and forth without attenuation. This phenomenon is common in short and flat canals with low friction, since it takes longer for the energy of the wave to dissipate. This phenomenon is not seen in the case of the Corning canal.

In both canals, the phase plot starts at −90 degrees due to the integrator, and then it decreases due to the time delay.

All models are good in low frequencies: in the gain plot, they have the straight line with the same slope and in the phase plot they start at −90 degrees. As was seen in the step responses, only the ID and the IDZ approximates the time delay well. All models except the IDZ underestimate the high frequency gain. In both cases the FO model gives the lowest estimate. The IDZ model approximates the high frequency gain better than the other models, specially in the case of the Corning canal. However, in the case of the laboratory canal, it is crossing the resonance peaks: at some frequencies it estimates the gain lower and at some other frequencies it estimates the gain higher than the real value.

Evaluation of the time and frequency domain comparison

While some models show good performance in the time domain, some others show good performance in the frequency domain. Some of them are able to approximate one property as, for instance, the time delay in the case of ID and IDZ models, the shape of the time response (FO model), or the high frequency behavior (IDZ model). From these properties, it is not straightforward to conclude which model will serve better as internal model for predictive control design. In the following, controllers based on all four models are implemented and their performance is analyzed to demonstrate a broader perspective for such a conclusion.

PREDICTIVE CONTROLLER DEVELOPMENT

The state space models

In order to develop predictive controllers, a discrete time state space model is obtained from the continuous models using discretization time steps of 500 s and 10 s for the Corning canal and the UPC-PAC, respectively. A state space model is developed for each hydraulic model with the same following form

$$x(k+1) = Ax(k) + Bu(k) + B_{\mathrm{d}}W(k) \tag{22}$$

where $x(k)$ is the state vector, $u(k)$ is the input control vector, $W(k)$ is the disturbance vector, and A, B, B_{d} are matrices of appropriate dimensions. The index k counts time steps. The state contains the errors in water depths

and discharges in the past instants, while the input variable is the change in discharge (Δq_{in})

$$x(k) = \begin{bmatrix} q_{in}(k) \\ q_{in}(k-1) \\ \dots \\ e(k) \\ e(k-1) \end{bmatrix} \quad (23)$$

$$u(k) = \Delta q_{in}(k). \quad (24)$$

The water depth error is defined as the difference between the water depth and the setpoint

$$e(k) = h(k) - h_{sp}(k) \quad (25)$$

The disturbance vector *W(k)* contains the known disturbances, which are offtake discharges (q_{off}) located close to the downstream end of the canal. Therefore they affect the downstream water depth without delay. The discharge q_{off} can be expressed by any of the models considered in this paper, using the same expressions used to model q_{out}.

The downstream boundary condition is implemented by linearizing the weir or the gate equation

$$Q_{gate} = C_{dg} L_g B_g \sqrt{2g(H - H_2)} \quad (26)$$

where for a rectangular cross section, C_{dg} is the gate discharge coefficient, B_g is the gate width, L_g is the gate opening, and H_2 is the water depth downstream of the gate. In this case the gate opening is constant and the downstream water depth is assumed to be constant, therefore the linearized equation has only one variable, the relative water depth (h) at the downstream end of the pool

$$q_{gate} = k_{hg} h \quad (27)$$

where k_{hg} is the gain of the gate discharge, which can be calculated as the derivative of the gate equation with respect to the water level upstream of the gate. The same procedure is valid if there is a weir at the downstream end of the canal. The weir equation is the following:

$$Q_{weir} = \frac{2}{3} C_{dw} L_w \sqrt{2g} (H - O)^{3/2} \quad (28)$$

where C_{dw} is the weir discharge coefficient, L_w is the weir width, and O is the weir height. This equation can be linearized and the constants can be joined in a single gain factor

$$q_{weir} = k_{hw} h \quad (29)$$

where k_{hw} is the gain of the weir discharge and can be calculated by differentiating the weir equation with respect to the water depth. The gate and weir equations were linearized when the model was constructed. Linearizing at every control step would improve the procedure.

Therefore the output discharge can be modeled in the form

$$\frac{q_{out}(s)}{h(s)} = k_h \quad (30)$$

where k_h is either k_{hw} or k_{hg} depending on whether there is a gate or weir at the downstream end of the canal. More details about the state space formulation are found in Horváth *et al.* (2014).

The predictive controller

A predictive controller has been developed based on the work carried out by Martín Sánchez & Rodellar (1996). The objective of the predictive controller is to keep the downstream water depth at the setpoint. The control action variable is the discharge under the upstream gate. As a first step, the optimization is carried out resulting in an upstream discharge value as solution.

In a second step, a gate inverse formula is used to calculate the gate opening as a function of the flow (calculated by the optimization) and the difference between the water depth at the upstream and downstream side of the gate (from the measured values). The controlled variable is the water depth downstream in the pool.

To obtain the control law, in order to keep the process output as close as possible to a predefined reference, an optimization process is carried out over a prediction interval $[k, k+\lambda]$, where k is the present time instant and λ is the prediction horizon. This optimization is defined by the

minimization of the following cost function:

$$\min_{\Delta q_{\text{in}}} J = \sum_{j=0}^{\lambda} \left\{ e^{\text{T}}(k+j|k) P e(k+j|k) \right\} + \sum_{j=0}^{\lambda} \left\{ \Delta q_{\text{in}}^{\text{T}}(k+j|k) R \Delta q_{\text{in}}(k+j|k) \right\} \quad (31)$$

where superscript T means transpose of the matrix, P is the weighting matrix for the water depth error, R is the input (change in upstream discharge) weighting matrix, and $(k+j|k)$ denotes that the value of the corresponding variable is predicted at the current instant k for a future instant $k+j$. Based on a simple linear model, that is referred to as internal model, the controller predicts the future output values as a function of past values of inputs and outputs and future control signals. These predictions are substituted to the cost function J, obtaining an expression whose minimization leads to the looked-for values. The first control action $\Delta q_{\text{in}}(k|k)$ is sent to the gates while the rest are neglected. At the next sampling time, the system is updated by measurements and the optimization process is repeated with new values. Details about the formulation of the controller can be found in Martín Sánchez & Rodellar (1996), Gómez *et al.* (2002), and van Overloop (2006). The details of the controller tuning are presented in Appendix B (available online at http://www.iwaponline.com/jh/016/110.pdf).

The variable calculated from the predictive controller is the change in the input discharges. There are different possibilities to obtain the gate opening from the calculated discharge: use another controller (for example a PID) with a faster sampling rate, use the inverse gate equation with the current water levels, or use the inverse gate equation by using the predicted water levels for the following time step (Malaterre & Baume 1999). In this work, the simplest approach is used, as it is commonly used in the literature (Deltour 1992; Schuurmans 1997); the new gate openings are calculated by using the inverse of the gate equation. It might also be beneficial to use the gate openings directly as control action variable. However, this problem is not investigated in this work, but is addressed in Horváth (2013).

The test cases

Two scenarios were tested for the canals: (1) a setpoint change; and (2) a known disturbance produced by opening an offtake weir. For the Corning canal, the scenario was 20 h long, and at 5 h a setpoint change (2.1 to 2.2 m) or a disturbance occurred (1 m^3/s was pumped from the downstream end of the canal). This amount of offtake is less than 10% of the total discharge; it corresponds to the benchmark tests presented in Clemmens *et al.* (1998). In all cases, these changes were known beforehand for the controller. In the case of the laboratory canal, the two scenarios are 40 min long, and the setpoint change (from 65 to 70 cm) occurs at 10 min, as well as the disturbance: a gravity offtake was opened at 45 m distance from the downstream end of the canal and about 23 L/s discharge was taken, that is about 40% of the total discharge. The offtake discharges represent the lateral offtake of a real irrigation canal. The tests are designed for normal canal operation conditions, and it might be also interesting to investigate the response of the controller in more extreme situations, or several canal pools using different configurations. The downstream boundary condition was the hydraulic structure: a weir for the UPC-PAC and gate for the Corning canal.

The efficiency of the controllers is analyzed by using the performance indices suggested by the ASCE (Clemmens *et al.* 1998) and often used (e.g., Malaterre 1998; Wahlin 2004), which are three indicators computed for each controlled variable (downstream water depth).

The maximum absolute error (MAE) is the maximum difference in percentage between the observed and the target water level

$$MAE = \frac{\max\left(\left|y_{\text{measured}} - y_{\text{target}}\right|\right)}{y_{\text{target}}}, \quad (32)$$

where y_{measured} is the measured water level and y_{target} is the target water level. The integral of the absolute magnitude of the error (IAE) gives information about the average performance of the controller during the whole simulation period (T_s)

$$IAE = \frac{\frac{\Delta t}{T_s} \sum_{t=0}^{T_s} \left|y_{\text{measured}} - y_{\text{target}}\right|}{y_{\text{target}}}. \quad (33)$$

While IAE is calculated over all the simulation period, the steady state error (StE) is the maximum difference

between the target and the actual water level during the last period of the test when the steady state should already be reached

$$StE = \frac{\max\left(\left|\bar{y}_{\text{measured}*} - y_{\text{target}}\right|\right)}{y_{\text{target}}}, \tag{34}$$

where $\bar{y}_{\text{measured}*}$ is the average of the measured water level in the period when the controller has already reached the new setpoint. In the case of the Corning canal, the last 2 hours are considered and in the UPC-PAC the last 10 minutes. TSS indicator is the time it takes for the water level to reach the steady state within 1.5% of maximum deviation from the target level

$$\rho = \left\{ t \middle| \forall \sigma \geq t \Rightarrow \frac{\max\left(\left|y_t - y_{\text{target}}\right|\right)}{y_{\text{target}}} < 0.015 \right\}, \tag{35}$$

$$TSS = \min_t \rho. \tag{36}$$

The SIC software (simulation of irrigation canals) is a hydraulic simulation software adapted to the calculation of flows in irrigation canals developed by IRSTEA, formerly Cemagref (Malaterre & Baume 1997). The SV equations are solved numerically using the Preissmann scheme, an implicit finite difference scheme.

RESULTS AND DISCUSSION

MPC is implemented based on the four above-mentioned models. The performance of these controllers is compared through test cases and the errors between the desired water levels and the actual water levels achieved by the controller are reported. First the results for the Corning canal and then the numerical and experimental results for the UPC-PAC are discussed.

Results by controlling the first pool of the Corning canal

Model predictive controllers were developed based on the four different models and numerically implemented on the first pool of the Corning canal as an example of Type 3 canals from the Cemagref benchmark. The results of the setpoint change and disturbance tests are discussed below.

Figure 6 shows a setpoint change of 10 cm that occurred at 5 h in the Corning canal. The MPC-FO has unacceptably bad performance: the water depth rises 50 cm higher than the setpoint when a change of 10 cm was required and relaxes after 10 h. The MPC-MUS has a considerably bad performance, showing an overshoot of 15 cm and returns to setpoint after 4 h. MPC-ID and MPC-IDZ perform well, without overshoot, and the new setpoint is reached within 2 h.

Figure 7 shows the disturbance test for the Corning canal. All models except MPC-FO have a similar performance: the disturbance occurs at 5 h. In all the cases, the controller first increases the water depth preparing for the extra offtake and then the water depth drops when the offtake opens (5 h). The setpoint is recovered within 3 h without oscillation in the case of the three controllers.

Table 3 shows the performance indicators related to this test. The results for the setpoint change clearly show that MPC-ID and MPC-IDZ gave satisfactory results, reaching the setpoint faster than the other two controllers, with MPC-FO exhibiting the worst behavior. For the disturbance test, most of the results have similar order of magnitude, only the MPC-FO showing a worse performance. In this case the water level (except for MPC-FO) stays in the

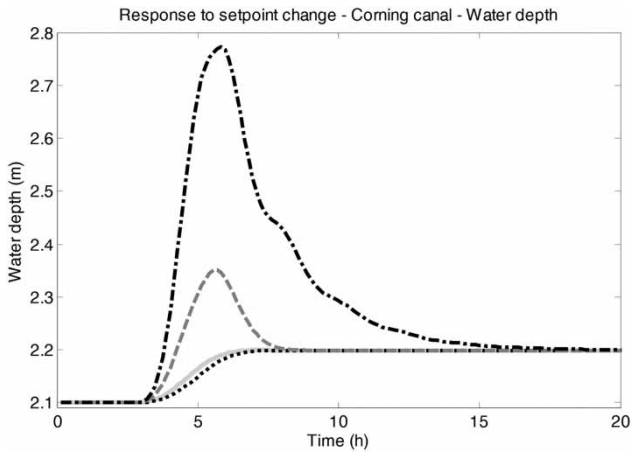

Figure 6 | Comparison of the simulation of controlled water depth by four different controllers in the Corning canal during a setpoint change experiment; the setpoint was changed at 5 h from 2.1 m to 2.2 m: MPC-ID (solid gray line), MPC-IDZ (dotted black line), MPC-MUS (dashed gray line), and MPC-FO (dash-dot line).

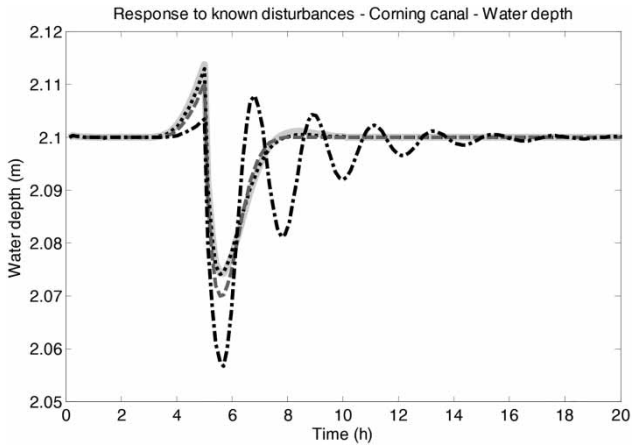

Figure 7 | Comparison of the simulation of controlled water depth by four different controllers in the Corning canal when a disturbance occurs (the offtake discharge is increased by 1 m^3/s at the downstream end); the disturbance occurred at 5 h from 2.1 m to 2.2 m: MPC-ID (solid gray line), MPC-IDZ (dotted black line), MPC-MUS (dashed gray line) and MPC-FO (dash-dot line).

Table 3 | Performance indicators (percentage) using four different controllers for setpoint change and disturbance rejection test on the Corning canal

	Setpoint change				Disturbance rejection			
	MAE	IAE	StE	TSS	MAE	IAE	StE	TSS
MPC-ID	2.75	0.22	0.10	5	1.22	0.11	0.00	0
MPC-IDZ	2.35	0.24	0.11	5.4	1.23	0.10	0.00	0
MPC-MUS	8.97	0.94	0.09	7	1.43	0.10	0.00	0
MPC-FO	26.05	4.93	0.02	12.6	2.06	0.19	0.01	6

MAE = maximum absolute error, IAE = integral of absolute magnitude of error, StE = steady state error, TSS = time to reach the steady state (hours).

range of 1.5% difference, so the time to reach this bound is zero. These observations coincide with the conclusions drawn from the figures.

For the Corning canal, in general MPC-ID and MPC-IDZ showed good performance, while the other two controllers (MPC-MUS and MPC-FO) did not show acceptable performance in all cases. The unsatisfactory performance of the FO model can be explained by the low number of moments to be matched. Recently, Litrico *et al.* (2010) suggested a solution for the extreme cases when $C_L < 1$, that is the canal pool is extremely short, so the time constant can be forced to be zero and the system can be modeled as a pure time delay. This approach resulted in the ID model.

For canals of this type (Type 3 in the Cemagref benchmark, i.e., FO system without resonance), the MPC-ID and MPC-IDZ controllers can give good performances. This type of canal can be modeled with both of these simple linear models. As significant performance differences were not observed, the ID model is preferable since it is easier to build.

Numerical results for the UPC-PAC

The four controllers were implemented numerically on the UPC-PAC and the best ones were further tested experimentally. First the results of the numerical tests, and then the results of the experimental tests are discussed. Figure 8 shows a setpoint change test. The results are similar to those of the Corning canal, that is MPC-MUS and MPC-FO controllers have unacceptable performance, while both MPC-ID and MPC-IDZ perform well.

Figure 9 shows a disturbance test on the UPC-PAC canal. Within 20 min, all controllers reach a 5 mm range from the setpoint. MPC-IDZ and MPC-MUS recover in 15 min, but MPC-MUS recovers through some oscillations. MPC-ID has no oscillations at all, but it is the slowest taking 30 min to recover. Table 4 presents the performance indicators. For the setpoint change test, the table values show the same tendency as observed in Figure 8: MPC-MUS and MPC-FO controllers are clearly the worst, MPC-ID and MPC-IDZ have the same order of magnitude, and MPC-ID is the best. For the disturbance test, all the values have similar order of magnitude.

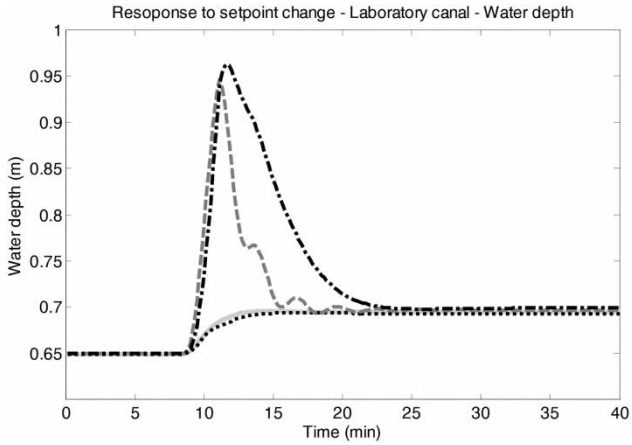

Figure 8 | Comparison of the simulation of controlled water depth by four different controllers in UPC-PAC during a setpoint change experiment, the setpoint was changed at 10 min from 0.65 to 0.7 m: MPC-ID (solid gray line), MPC-IDZ (dotted black line), MPC-MUS (dashed gray line), and MPC-FO (dash-dot line).

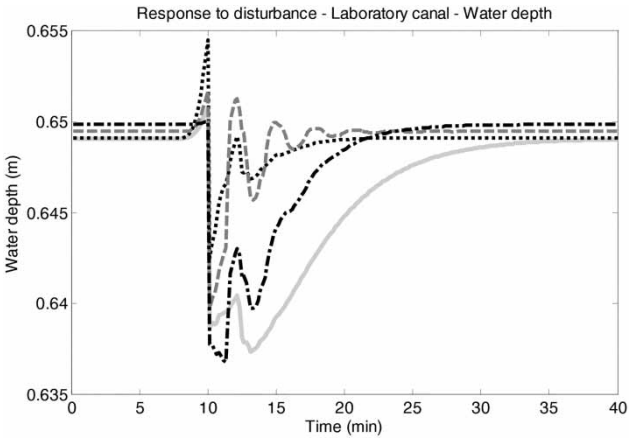

Figure 9 | Comparison of the simulation of controlled water depth by four different controllers in the UPC-PAC, at 10 min an offtake was opened and 25 L/s discharge was taken from the canal: MPC-ID (solid gray line), MPC-IDZ (dotted black line), MPC-MUS (dashed gray line), and MPC-FO (dash-dot line).

The difference between the two responses can also be seen in Figure 9: while the response of the MPC-ID controller is slow, the response of MPC-IDZ is faster with some oscillations. This fact might be the cause of the difference between the MAE (it reaches a bigger extreme in the case of the MPC-ID). Let us note that this difference is 1.15 and 1.95%, less than half a centimeter. Similar observations can be added for the integral absolute error: for MPC-ID it is 0.54% and for MPC-IDZ it is 0.19%. The difference is very small and the reason is the different nature of the responses. The steady state was reached between 10 and 20 min for all models. For the setpoint change test, the MPC-ID controller was the fastest to reach the steady state, then the other controllers MPC-IDZ, MPC-MUS, and MPC-FO increasing the time to reach it. In the case of the disturbance test, the MPC-IDZ was the fastest and the MPC-ID was the slowest.

Based on these results, experiments are designed to test the controllers in a real environment. While for the disturbance test, the performance of all controllers was acceptable, the setpoint test clearly shows that for the UPC-PAC only the MPC-ID and MPC-IDZ are worthy of further testing.

Experimental results on the canal UPC-PAC

The controllers were implemented in the laboratory canal UPC-PAC. The canal has a supervisory control and data acquisition system (SCADA) developed in Matlab/Simulink environment (Mathworks 2008). Hence, the control algorithm only has to be programmed in Embedded Matlab language and then it can directly be tested on the canal. The measurement data from the water depths and the gate openings are processed by the SCADA system and the control actions are sent to the gates. The best performing controllers (MPC-ID and MPC-IDZ) were implemented in the laboratory and tested experimentally. The following results are the measured values of the water levels from the SCADA system of the laboratory canal.

Figure 10 shows the results of the setpoint change test. Both MPC-ID and MPC-IDZ were able to control the water level in the same manner. The water levels are within a range of 0.5 cm around the setpoint. Figure 11 shows the reaction to known disturbances. Both MPC-ID and MPC-IDZ were able to control the water level in the same manner. The water levels are within a range of 0.5 cm around the setpoint. Both MPC-ID and MPC-IDZ were implemented successfully in the UPC-PAC experimental facility.

Table 5 shows that both MPC-ID and MPC-IDZ were able to control the UPC-PAC. The experiments showed

Table 4 | Performance indicators (in percentage) using four different controllers for setpoint change and disturbance rejection test on the UPC-PAC canal

	Setpoint change				Disturbance rejection			
	MAE	IAE	StE	TSS	MAE	IAE	StE	TSS
MPC-ID	3.94	0.71	0.72	11.8	1.95	0.54	0.17	16.7
MPC-IDZ	4.19	0.91	0.96	13	1.15	0.19	0.14	0
MPC-MUS	35.16	2.65	0.43	15.1	1.58	0.15	0.08	10.7
MPC-FO	37.53	4.86	0.14	20.1	2.03	0.28	0.03	14

MAE = maximum absolute error, IAE = integral of absolute magnitude of error, StE = steady state error, TSS = time to reach the steady state (min).

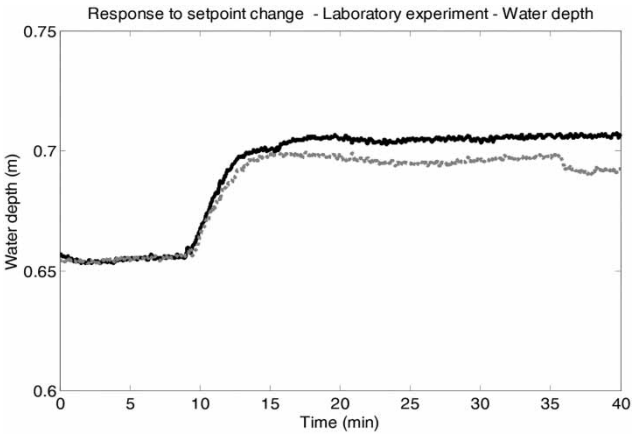

Figure 10 | Comparison of measured water depth in the UPC-PAC during a setpoint change experiment: the setpoint was changed at 10 min from 65 cm to 70 cm. Two different implemented controllers: solid line the MPC-ID and dashed line the MPC-IDZ.

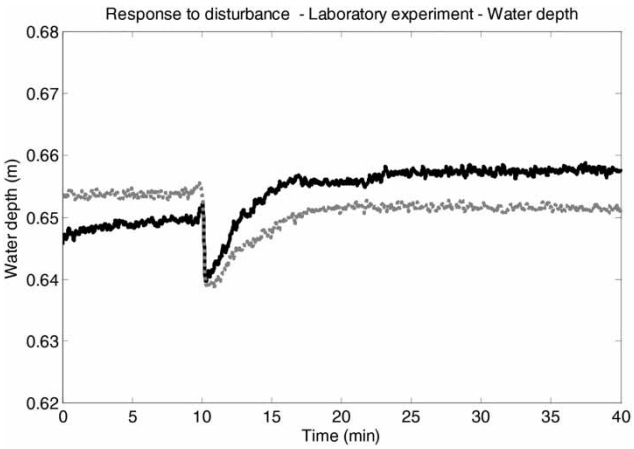

Figure 11 | Comparison of measured water depth in the UPC-PAC during a known disturbance experiment: 10 min 30 L/s discharge offtake opened (the canal discharge was increased from 60 to 90 L/s. Two different implemented controllers: solid line the MPC-ID and dashed line the MPC-IDZ.

Table 5 | Performance indicators (percentage) using the MPC-ID and MPC-IDZ controllers for setpoint change and disturbance rejection experiment on the UPC-PAC canal

	Setpoint change				Disturbance rejection			
	MAE	IAE	StE	TSS	MAE	IAE	StE	TSS
MPC-ID	4.65	0.82	0.84	11.8	1.59	0.78	1.13	10.7
MPC-IDZ	4.99	0.81	0.71	12.6	1.76	0.40	0.22	11.5

MAE = maximum absolute error, IAE = integral of absolute magnitude of error, StE = steady state error, TSS = time to reach the steady state (min).

that the MAE is less than 5% with both models for the setpoint change test, and less than 2% for the disturbance rejection test. The steady state error is about 1%. The steady state was reached slightly, but not considerably faster in the case of the ID model.

The experimental results confirm those of the numerical tests. In the experimental results, the water levels have steady state offset; there is always about 0.5 cm difference between the actual water level and the setpoint. Both controllers have acceptable test results given the constraints of the facility, which are: (1) the minimum gate movement is 2 mm; and (2) the water level measurement error is 10 mm. For the disturbance rejection test, the water level moved less than 2 cm and the discharge increased as a step without excessive gate movements.

Both MPC-ID and MPC-IDZ were able to control a canal of Type 1, a short canal prone to resonance. It is important to mention that these two controllers gave good performance with sufficiently loose tuning, in order to avoid instability of the controller. Alternative ways to address the control of resonance-sensitive canals can be to filter out the resonance (Schuurmans 1997; Horváth *et al*. 2014) or include the resonance in the modeling stage (van Overloop *et al*. 2010b; Horváth 2013).

Both canals examined were short, having FO behavior, and one of them being resonant. In the case of the resonant canal, the resonance should be taken into account. Here, only a less strict tuning was considered with respect to this problem. The control of this kind of canal pool can be more efficient using models especially developed for this specific kind of canal pool.

On computational efficiency

For the implementation of the predictive controllers, a linear quadratic optimization problem is solved at each discrete-time control instant. The size of this problem has a direct influence on the execution time of the controller. In this case, the size of the matrices in the optimization problem is the model dimension multiplied by the length of the prediction horizon measured in number of time steps. For the ID and IDZ models, the system has a dimension 13, while in the case of the MUS and FO models the system has a dimension of 5. This difference is more than double,

which can increase the execution time. However, it is important to mention that in both cases the execution time is significantly small in comparison to the control time step, especially in the case of the Corning canal. Although with current settings the ID and IDZ models require longer execution time, for the purpose of the application this does not cause a disadvantage.

Generalization of the findings

The ID and IDZ models gave good performance for two example canals belonging to Cemagref benchmark canal Types 1 and 3. While the waves in the UPC-PAC are under-damped, they are damped in the Corning canal. As to the order of the system, both canals belong to FO systems. The other canal types define canals whose behavior can be modeled with second order or second order with time delay. These might show better results with other modeling approaches. For example, Litrico & Georges (1999) show a good time domain model for a canal of second order with delay. Therefore, the findings cannot be generalized to all canal types in a straightforward manner. More numerical test and time and frequency domain analysis would be needed to extend these results.

CONCLUSION

Four simplified models (Muskingum, FO model based on the Hayami equation, ID and IDZ) have been compared for control purposes on two different types of short canal. The comparison has been based on MPC of one canal pool. The comparison could be further extended by using several canal pools and different configurations. The results show that the performance of the controller is significantly influenced by the choice of the model. From the simulation and experimental results, only the ID and IDZ models proved to be acceptable on these two example canals. One is a laboratory canal, very short and flat, prone to resonance; the other is the first pool of the Corning canal, which is relatively long and flat. Both canals belong to the group of canals characterized by FO behavior.

The range of validity of the conclusions drawn in this work can be extended to two of the canal families characterized by the Cemagref benchmark. One is the so-called Type 1, which exhibits a FO dynamics with resonance. The other is the so-called Type 3, which is a FO system without resonance. A similar procedure can be adopted to study different canal types.

REFERENCES

Aguilar, J., Langarita, P., Linares, L. & Rodellar, J. 2009 Automatic control of flows and levels in an irrigation canal. *IEEE Trans. Ind. Appl.* **45** (6), 2198–2208.

Aguilar, J., Langarita, P., Linares, L., Galvis, E., Horvath, K., Rodellar, J. & Gómez, M. 2011 Control automático de niveles en un canal experimental dividido en tres tramos (Automatic control of water levels in a three-reach laboratory canal). In JIA 2011. II Jornadas del Ingeniería del agua, Modelos numéricos en dinámica fluvial, Barcelona, Spain.

Aguilar, J. V., Langarita, P., Linares, L., Rodellar, J. & Soler, J. 2012 Adaptive predictive expert control of levels in large canals for irrigation water distribution. *Int. J. Adapt. Control* **10** (26), 945–960.

Alvarez Brotons, X. 2004 *Control Predictivo de Canales de Riego Utilizando Modelos de Predicción de Tipo Muskingum (primer orden) y de Tipo Hayami (segundo orden)* (*Predictive control of irrigation canals using Muskingum (first order) and Hayami (second order) models*). Minor Thesis, Technical University of Catalonia, Spain.

Baume, J.-P. & Sau, J. 1997 Study of irrigation canal dynamics for control purposes. In: *Int. Workshop on the Regulation of Irrigation Canals, RIC*, Marrakech, Morocco, pp. 3–12.

Baume, J.-P., Sau, J. & Malaterre, P.-O. 1998 Modelling of irrigation channel dynamics for controller design. In: *Proceedings of Systems, Man and Cybernetics '98*, San Diego, CA, pp. 3856–3861.

Begovich, O., Ruiz, V., Besancon, G., Aldana, C. & Georges, D. 2007 Predictive control with constraints of a multi-pool irrigation canal prototype. *Lat. Am. Appl. Res.* **37** (3), 177–185.

Bryson, A. & Ho, Y. 1969 *Applied Optimal Control: Optimization, Estimation, and Control*. Hemisphere Publishing Corporation, Washington, DC, USA.

Charbonnaud, P., Carrillo, F. J. & Duviella, E. 2011 A supervised robust predictive multi-controller for large operating conditions of an open-channel system. In: *IFAC World Congress*, Milano, Italy, August 28–September 2.

Chentouf, B. 2001 Robust regulation of a river reach governed by Hayami model. In: *Proceedings of the 40th IEEE Conference on Decision and Control*, Orlando, USA, pp. 4962–4967.

Chow, V. T. 1959 *Open-Channel Hydraulics*. McGraw-Hill Book Co. Inc., New York, USA.

Clemmens, A. J., Kacerek, T., Grawitz, B. & Schuurmans, W. 1998 Test cases for canal control algorithms. *J. Irrig. Drain. Eng.* **124** (1), 23–30.

Cunge, J. A. 1969 On The subject of a flood propagation computation method (Muskingum method). *J. Hydraul. Res.* **7**, 205–230.

Deltour, J.-L. 1992 *Application de l'Automatique Numérique à la Régulation des Canaux; Proposition d'une Méthodologie D'étude*. PhD Thesis, Grenoble Institute of Technology, France.

Duviella, E., Blesa, J., Bako, L., Bolea, Y., Sayed-Mouchaweh, M., Puig, V. & Chuquet, K. 2013 Inland navigation channel model: Application to the Cuinchy-Fontinettes reach. In: *The 10th IEEE International Conference on Networking, Sensing and Control*, Paris, France, April 10–12.

Eurén, K. & Weyer, E. 2007 System identification of open water channels with undershot and overshot gates. *Control Eng. Pract.* **15** (7), 813–824.

Gómez, M., Rodellar, J., Vea, F., Mantecón, J. & Cardona, J. 1998 Decentralized predictive control of multi-reach canals. In: *Proceedings of Systems, Man and Cybernetics '98*, San Diego, CA, pp. 3885–3890.

Gómez, M., Rodellar, J. & Mantecón, J. 2002 Predictive control method for decentralized operation of irrigation canals. *Appl. Math. Model.* **26**, 1039–1056.

Hayami, S. 1951 On the propagation of flood waves. *Bulletins-Disaster Prevention Research Institute*, Kyoto University **1**, 1–16.

Horváth, K. 2013 *Model Predictive Control of Resonance Sensitive Irrigation Canals*. PhD Thesis, Technical University of Catalonia, Spain.

Horváth, K., van Overloop, P. J., Galvis, E., Gómez, M. & Rodellar, J. 2014 Multivariable model predictive control of water levels on a laboratory canal. *Advances in Hydroinformatics*. Springer, Singapore, pp. 77–92.

Igreja, J. & Lemos, J. M. 2009 Nonlinear model predictive control of a water distribution canal pool. In International Workshop on Assessment and Future Directions of Nonlinear Model Predictive Control, Pavia, Italy, **384**, 521–529, Springer.

Litrico, X. & Fromion, V. 2004a Analytical approximation of open-channel flow for controller design. *Appl. Math. Model.* **28**, 677–695.

Litrico, X. & Fromion, V. 2004b Frequency modeling of open-channel flow. *J. Hydraul. Eng.* **130** (8), 806–815.

Litrico, X. & Fromion, V. 2004c Simplified modeling of irrigation canals for controller design. *J. Irrig. Drain. Eng.* **130** (5), 373–383.

Litrico, X. & Georges, D. 1999 Robust continuous-time and discrete-time flow control of a dam-river system. (I) Modelling. *Appl. Math. Model.* **23**, 809–827.

Litrico, X., Pomet, J.-B. & Guinot, V. 2010 Simplified nonlinear modeling of river flow routing. *Adv. Water Resour.* **33**, 1015–1023.

Malaterre, P.-O. 1994 *Modelisation, Analysis and LQR Optimal Control of an Irrigation Canal*. PhD Thesis, LAAS-CNRS-ENGREF-Cemagref, France.

Malaterre, P.-O. 1998 PILOTE: Linear quadratic optimal controller for irrigation canals. *J. Irrig. Drain. Eng.* **124** (4), 187–194.

Malaterre, P.-O. 2008 Control of irrigation canals: Why and how? In: *Proceedings of the International Workshop on Numerical Modelling of Hydrodynamics for Water Resources*, Zaragoza, Spain, pp. 271–292.

Malaterre, P.-O. & Baume, J. P. 1997 SIC 3.0, a simulation model for canal automation design. In: *International Workshop on Regulation of Irrigation Canals: State of art of research and applications*, Marrakech, Morocco (A. Mokhlisse, ed.), pp. 68–75.

Malaterre, P.-O. & Baume, J.-P. 1998 Modeling and regulation of irrigation canals: existing applications and ongoing researches. In: *IEEE International Conference on Systems, Man, and Cybernetics 1998*, San Diego, California, USA, vol. 4, pp. 3850–3855.

Malaterre, P.-O. & Baume, J. P. 1999 Optimum choice of control action variables and linked algorithms: Comparison of different alternatives. In: *Proceedings of USCID Workshop on Modernization of irrigation water delivery systems*, Phoenix, Arizona, USA, pp. 387–405.

Malaterre, P. O. & Rodellar, J. 1996 Design and comparison of multivariable optimal and predictive controllers on a 2-pool irrigation canal. In *Journées Hispano-Françaises Systèmes Intelligents & Contrôle Avancé*, Laboratoire Européen Associé, Barcelona, Spain.

Mantecón, J. A., Gómez, M. & Rodellar, J. 2002 A Simulink-based scheme for simulation of irrigation canal control systems. *Simulation* **78** (8), 485–493.

Mareels, I., Weyer, E., Ooi, S., Cantoni, M., Li, Y. & Nair, G. 2005 Systems engineering for irrigation systems: Successes and challenges. *Annual Reviews in Control* **29** (2), 191–204.

Martín Sánchez, J. M. & Rodellar, J. 1996 *Adaptive Predictive Control – From Concepts to Plant Optimization*. Prentice Hall, Hertfordshire, UK.

Mathworks 2008 Matlab. http://www.mathworks.com/products/matlab/.

Ogata, K. 2010 *Modern Control Engineering*, 5th edn., Prentice Hall, Upper Saddle River, NJ, USA.

Ooi, S. K. & Weyer, E. 2001 Closed loop identification of an irrigation channel. In Proceedings of the 40th IEEE Conference on Decision and Control, Orlando, Florida, USA, vol. 5 pp. 4338–4343.

Puig, V., Quevedo, J., Escobet, T., Charbonnaud, P. & Duviella, E. 2005 Identification and control of an open-flow canal using LPV models. In: *Conference on Decision and Control and European Control Conference 2005*, Seville, Spain, pp. 1893–1898.

Refsgaard, J. C. 1996 Terminology, modelling protocol and classification of hydrological model codes. In: *Distributed Hydrological Modelling* (M. B. Abbot & J. C. Refsgaard, eds). Kluwer Academic Publishing, Dordrecht, The Netherlands, pp. 17–40.

Rodellar, J., Gómez, M. & Vide, J. 1989 Stable predictive control of open-channel flow. *J. Irrig. Drain. Eng.* **115** (4), 701–713.

Rodellar, J., Gómez, M. & Bonet, L. 1993 Control method for on-demand operation of open-channel flow. *J. Irrig. Drain. Eng.* **119**, 225–241.

Sawadogo, S. 1992 *Modelisation, Commande Predictive et Supervision d'un Systeme D'irrigation* (*Modelling, predictive*

control and supervision of an irrigation system). PhD Thesis, Paul Sabatier University, France.

Schuurmans, J. 1995 Open-channel flow model approximation for controller design. *Appl. Math. Model.* **19** (9), 525–530.

Schuurmans, J. 1997 *Control of Water Levels in Open Channels*. PhD Thesis, Delft University of Technology, The Netherlands.

Schwanenberg, D., Verhoeven, G. & Raso, L. 2010a Nonlinear model predictive control of water resources systems in operational flood forecasting. In Operational Flood Forecasting, 55th Internationales Wissenschaftliches Kolloqium, Ilmenau, Germany, 13–17 September 2010.

Schwanenberg, D., Verhoeven, G., van den Boogaard, H. & van Overloop, P.-J. 2010b Nonlinear model predictive control of flood detention basins in operational flood forecasting. In 9th International Conference on Hydroinformatics, HIC 2012.

Sepúlveda, C. 2008 *Instrumentation, Model Identification and Control of an Experimental Irrigation Canal*. PhD Thesis, Technical University of Catalonia, Spain.

van Overloop, P.-J. 2006 *Model Predictive Control on Open Water Systems*. PhD Thesis, Delft University of Technology, The Netherlands.

van Overloop, P.-J. & Bombois, X. 2012 Identification of properties of open water channels for controller design. In: *IFAC Symposium on System Identification*, Brussels, Belgium, vol. **16**, pp. 1019–1024.

van Overloop, P.-J., Schuurmans, J., Brouwer, R. & Burt, C. 2005 Multiple-model optimization of proportional integral controllers on canals. *J. Irrig. Drain. Eng.* **131** (2), 190–196.

van Overloop, P.-J., Weijs, S. & Dijkstra, S. 2008 Multiple model predictive control on a drainage canal system. *Control Eng. Pract.* **16**, 531–540.

van Overloop, P.-J., Clemmens, A. J., Strand, R. J., Wagemaker, R. M. J. & Bautista, E. 2010a Real-time implementation of model predictive control on Maricopa-Stanfield irrigation and drainage district's WM canal. *J. Irrig. Drain. Eng.* **136**, 747–756.

van Overloop, P.-J., Miltenburg, I. J., Bombois, X., Clemmens, A. J., Strand, R. & van de Giesen, N. 2010b Identication of resonance waves in open water channels. *Control Engineering Practice* **18** (8), 863–872.

van Overloop, P.-J., Horváth, K. & Aydin, B. E. 2014 Model predictive control based on an integrator resonance model applied to an open water channel identification of resonance waves in open water channels. *Control Eng. Pract.* **27**, 54–60.

Wahlin, B. & Clemmens, A. 2006 Automatic downstream water-level feedback control of branching canal networks: Theory. *J. Irrig. Drain. Eng.* **132** (3), 198–207.

Wahlin, B. T. 2004 Performance of model predictive control on ASCE Test Canal 1. *J. Irrig. Drain. Eng.* **130** (3), 227–238.

Weyer, E. 2001 System identification of an open water channel. *Control Eng. Prac.* **9** (12), 1289–1299.

Xu, M., van Overloop, P.-J. & van de Giesen, N. C. 2011 On the study of control effectiveness and computational efficiency of reduced Saint–Venant model in model predictive control of open channel flow. *Adv. Water Resour.* **34** (2), 282–290.

Zafra-Cabeza, A., Maestre, J. M., Ridao, M., Camacho, E. & Sánchez, L. 2011 Hierarchical distributed model predictive control for risk mitigation: An irrigation canal case study. In: *American Control Conference (ACC)*, 29 June–1 July, pp. 3172–3177.

Zhou, K. & Doyle, J. 1998 *Essentials of Robust Control*. Prentice Hall, Upper Saddle River, NJ, USA.

Zhuan, X. & Xia, X. 2007 Models and control methodologies in open water flow dynamics: A survey. In: *IEEE AFRICON 2007*, Windhoek, Namibia, 26–28 September 2007, pp. 1–7.

First received 2 October 2013; accepted in revised form 3 June 2014. Available online 1 July 2014